Sustainable Environment Research

RESEARCH

Open Access

Minimization of algogenic organic matter from cyanobacteria-laden water by electrochemical oxidation: molecular degradation signature of disinfection by-products precursors by electro-oxidation and electro-Fenton

Angga Aji[1,2], Fahrudin Sidik[1,2] and Jr-Lin Lin[1*]

Abstract

Algogenic organic matter (AOM) generated from cyanobacteria-impacted reservoirs poses a significant risk to drinking water. This study aimed to investigate the molecular degradation signature of *Microcystis aeruginosa* (MA)-derived AOM by electrochemical oxidation and the corresponding disinfection by-product formation potential (DBPFP). Boron-doped diamond (BDD)-based electro-oxidation (EO) and electro-Fenton (EF) were implemented at pH 3 and 10 mA cm^{-2} within 1 h. The fluorophore of extracellular organic matter (EOM), the mixture of EOM and intracellular organic matter (IOM), were characterized, and their corresponding molecular weight (MW) were fractionated. The results showed that dissolved organic carbon (DOC) degradation efficiency for BDD-EF treatment is superior and maintains DOC attenuation up to 84% for the EOM suspensions alone, while a low degradation efficiency occurs for IOM-EOM mixture. In contrast, BDD-EO exhibits a maximum DOC degradation around 66% for EOM suspensions alone, but DOC reduction is as low as 20% for IOM-EOM mixture. The H_2O_2 generated by BDD-EO preferentially degrades humic acid-like substances in EOM suspensions, whereas BDD-EF effectively degrades multiple fluorescent AOM by •OH. For IOM-EOM mixture, BDD-EO efficiently decomposes humics, but BDD-EF preferentially minimizes soluble microbial product-like and aromatic protein-like substances. Meanwhile, BDD-EF favors degrading biopolymers, humics, and low-MW substances, while BDD-EO merely degrades partial biopolymers and humic substances. After either EF or EO, specific DBPFP decreases as EOM presents alone where the toxicity of corresponding DBPs is mitigated effectively, instead the increased specific DBPFP appears for IOM-EOM mixture where the toxic potency ([DBP]/LC_{50}) of corresponding DBPs increases. In summary, EO and EF are powerful in attenuating MA-derived DBP precursors of EOM in the absence of IOM, depending on the molecular signature.

Keywords Algogenic organic matter, Cyanobacteria, Electro-oxidation, Disinfection-by-products

*Correspondence:
Jr-Lin Lin
jrlin@cycu.edu.tw
Full list of author information is available at the end of the article

1 Introduction

Cyanobacteria, particularly *Microcystis aeruginosa* (MA), are the most dominant species in water reservoirs. MA cells generally exhibit a higher growth rate than other algae during algae blooming in high nutrient-impact reservoirs. In eutrophicated reservoirs, algogenic organic matter (AOM), such as extracellular organic matter (EOM) and intracellular organic matter (IOM), predominantly exists during MA growth. At a decay or death phase, MA cells are in the condition of limited nutrient uptake, resulting in the occurrence of humification of AOM [1]. Meanwhile, it significantly causes the release of IOM and toxins into water bodies during photosynthetic activity. Both IOM and EOM are recognized as the precursors of carcinogenic disinfection by-products (DBPs), such as trihalomethanes (THMs) and haloacetic acids (HAAs), in chlorination process for drinking water supply [2, 3]. IOM mainly comprises aromatic and aliphatic substances which are composed of proteins, whereas EOM reflects humic-like characteristics [4]. AOM is essentially a heterogeneous mixture of nitrogenous compounds with high hydrophilic substances and lower aromatic contents compared to natural organic matter, leading to much more difficulty in removing AOM via conventional treatment processes [5]. Thus, the efficiency in AOM removal depends on its complexity of compositions and molecular fractions. In drinking water treatment, the IOM and EOM generated from eutrophicated reservoirs possess distinct compositional and molecular characteristics. The challenge of AOM removal increases significantly due to its dynamic reactivity in mixed IOM-EOM suspensions, particularly during cyanobacteria cell lysis. As a result, conventional water treatment processes are less efficient in separating AOM and their corresponding DBPs in cyanobacteria-impacted water.

Conventional water treatment processes, such as coagulation-sedimentation and sand filtration, effectively remove algal cells but fail to alleviate AOM due to its hydrophilic compounds [6]. Single and multiple doses of NaOCl and ClO_2 oxidants are commonly used to enhance cyanobacterial inactivation and minimize AOM in pre-oxidation where it can significantly deform algal cells and cause the release of IOM. It would be a major tradeoff for pre-oxidation-assisted coagulation, further raising concerns about DBP elevation upon post-chlorination [7, 8]. It has been proven that IOM of cyanobacteria is the dominant DBP precursor instead of EOM, especially for the formation of nitrogenous DBPs [3, 8, 9]. Previous studies have indicated that AOM with a low molecular weight (MW) ($<10^3$ Da) is insignificantly removed from cyanobacteria-laden water by conventional water treatment processes [1, 2]. To improve AOM degradation, advanced oxidation processes (AOPs), such as UV/H_2O_2/O_3, H_2O_2/Fe^{2+}, and H_2O_2/Fe^{2+}/UV have been proven its performance in the removal of EOM up to 95% [10, 11].

So far, electrochemical-oxidation processes (EOPs) have been extensively studied as an efficient, low chemical addition and broad-ecofriendly applicability to minimize the impact of harmful cyanobacterial blooms on drinking water sources [12, 13]. These electrochemical-oxidations reduce the use of toxic chemicals, leading to a reduced impact on the environment compared to conventional chemical treatment processes. The effectiveness of electro-oxidation (EO) and electro-Fenton (EF) depends on several essential parameters, such as electrode materials, reactor configuration, current density (CD), pH, and the types of concentration of electrolyte [14]. It has been reported that EF at pH 3.0 is effective in transforming small-molecule organics into other primary smaller molecules with the final products such as CO_2 and H_2O [15]. Boron-doped diamond (BDD) is a promising electrode for efficient organic matter reduction in bio-related compounds, pharmaceuticals, cyanotoxin removal, and various organic-rich wastewater treatment processes [13, 16]. For an EO process, BDD outperforms other anodes, such as platinum, titanium, graphite, and mixed metal oxides, in organic substance degradation, owing to its high overpotential to generate high-level H_2O_2 [17]. However, H_2O_2 typically lacks sufficient selectivity to oxidize organic compounds [18]. Unlike BDD-EO, previous studies have suggested that the removal efficiency of MA can reach over 95% by disintegrating cells with hydroxyl radicals (•OH) generated during BDD-EF reaction [19]. Although many studies have investigated the effectiveness of electrochemical oxidation on organic matter degradation in wastewater treatment, the direct degradation of MA-derived AOM by EO and EF is still under investigation for drinking water treatment, especially in the degradation of the mixed IOM-EOM suspensions. It is warranted to further study the molecular degradation behaviors of AOM by EO and EF in the presence and absence of IOM in order to evaluate the implications of electrochemical oxidation in cyanobacteria-impact water treatment.

This study aimed to investigate the performance of BDD-EO and BDD-EF processes for MA-derived AOM degradation towards EOM suspensions in the presence and absence of IOM. The generation of H_2O_2 and •OH were tested as well as the reduction in DOC and UV_{254} were measured during EO and EF within 1 h at CD as low as 10 mA cm^{-2}. Furthermore, the variations in the average fluorescent intensity (AFI) and MW were analyzed during EO and EF treatment on AOM suspensions. Finally, the DBP formation potential (DBPFP) towards AOM is determined to evaluate the significance of AOM composition in the EOPs for DBP precursors

degradation. Lastly, the molecular degradation signature of cyanobacteria-derived DBPs precursors by EO and EF was proposed.

2 Materials and methods

2.1 Chemicals and AOM sample preparation

Analytical grade chemicals, including sodium sulfate (Na_2SO_4), ferrous sulfate heptahydrate ($FeSO_4{\cdot}7H_2O$), sulfuric acid (H_2SO_4), sodium hydroxide (NaOH), potassium titanium oxalate dihydrate ($K_2TiO(C_2O_4)_2{\cdot}2H_2O$), terephthalic acid (THA, $C_6H_4(CO_2H)_2$), and potassium phosphate dibasic (K_2HPO_4), were purchased from Sigma-Aldrich (Germany). Graphite felt (Shenzhen Zhenzhixing Technology Co.) and BDD, Chenguang Machinery & Electric Equipment Co., China) were used as the cathode and anode, respectively.

The MA strains were cultivated in several 500 mL Erlenmeyer flasks containing BG-11 media. The temperature was set at room temperature (25 ± 1 °C) with a light cycle of 12:12 (day: night) at a continuous rotation of 100 rpm. Figure S1 shows the observation on the MA cell by scanning electron microscope (SEM) scanning at the stationary phase where the MA suspensions contain a total cell count of approximately 1×10^7 cells L^{-1}. Harvested AOM suspensions were then separated into EOM and IOM suspensions.

2.2 EOM and mixed IOM-EOM suspensions extraction

In order to obtain the EOM suspensions, the MA cell suspensions were first centrifuged at 4000 rpm for 15 min (DM0636, DLAB, United States). Then, the supernatant was filtered through a 0.45 µm mixed cellulose ester (MCE) membrane filter (Advantec, Japan). Eventually, the EOM suspension was obtained from filtered suspensions and stored at −20 °C before each test to prevent organic degradation [12]. Subsequently, the mixed IOM-EOM suspensions were extracted by subjecting the MA cell suspension to a brief preheating step at 60 °C for 10 min on a heating plate (DLAB, USA), following the same procedure as the extraction process of EOM suspensions. This thermal extraction method is more effective than centrifugation and chemical extraction using NaOH, resulting in strong absorbance spectra with negligible changes to their chemical compositions [20].

2.3 Protocol of electrochemical oxidation tests

The electrochemical oxidation tests were conducted in a 1-L beaker glass filled with 1 L of 20 mM Na_2SO_4 for BDD-EO, while a similar solution with the addition of 3 mM $FeSO_4{\cdot}7H_2O$ as the catalyst, was prepared for BDD-EF, as depicted in Fig. S2. The addition of Na_2SO_4 facilitates electron transfer during electrochemical oxidation in lab-scale experiments [19]. The BDD anode and graphite felt cathode with an active area of 26.2 cm^2 and an inter-electrode gap of 2 cm were connected to a direct current power supply device (CPS-3205, Gophert, Taiwan). The CD applied in EO and EF tests was maintained at 10 mA cm^{-2} following a previous study where the oxidizing agent was effectively generated to degrade algal cells and organic matter at a current density of 10 mA cm^{-2} in an BDD-based electrochemical oxidation process [12], and the operational pH (3, 7, and 8.5) was adjusted using H_2SO_4 or NaOH solution. A magnetic stirrer (DLAB, USA) was used at the bottom of the beaker to promote mixing at 60 rpm. Before each test, the electrodes were submerged in 0.1 M H_2SO_4 for 10 min and rinsed with ultrapure water and 95% ethanol, as previously described [21]. The stability test for BDD electrode was proceeded via cyclic voltammetry and electrochemical impedance spectroscopy (EIS) test. It shows a wide electrochemical stability window from −2 to 2 V vs. reversible hydrogen electrode and minimal background current, ensuring high resistance to side reactions. Additionally, EIS test confirms efficient electron transfer and excellent conductivity, with impedance values around 6–7 Ω (see Fig. S3). The similar BDD electrode reported by a previous study has exhibited a crystalline structure with grain sizes up to 10 µm, as observed by SEM, while the Raman spectra show B-B and C-B vibrations at approximately 460 and 1220 cm^{-1}, respectively [22]. The generation rate of H_2O_2 and •OH was evaluated in the absence of AOM suspensions, as shown in Fig. 1. Samples were periodically withdrawn and divided into two tubes. A 20 mL sample was mixed with 2.5 mL of 0.7 M H_2SO_4 and 2 mL of 0.02 mM potassium titanium oxalate for H_2O_2 measurement. A 9 mL sample was added to 1 mL of a probe mixture (5 mM NaOH and 2 mM THA) for OH radical measurement. A UV–Vis spectrophotometer (Genesys™ 10S, Thermo Scientific, USA) was used to measure H_2O_2 absorbance at 400 nm [23]. To determine the generation of •OH, 2D emission spectrum (Em) scanning was employed using a fluorescent spectrophotometer (RF-6000, Shimadzu, Japan). The •OH measurement was conducted at an emission wavelength of 425 nm and a scanning rate of 5 nm s^{-1}, as described previously [24]. Fluorescence-based measurements using the 2-hydroxyterephthalic acid chemical probe, as previously reported, are not affected by natural species such as inorganic ions (Cl^-, NH_4^+, and SO_4^{2-}) or organic compounds such as carboxylic acids (formic, succinic, and oxalic acids) in aqueous environment. This method is also considered more reliable compared to other chemicals like nitrobenzene and benzoic acid [25]. Calibration standards were prepared using THA at various concentrations (0.5, 1, 5, and 8 mg L^{-1}) and pH 3.5.

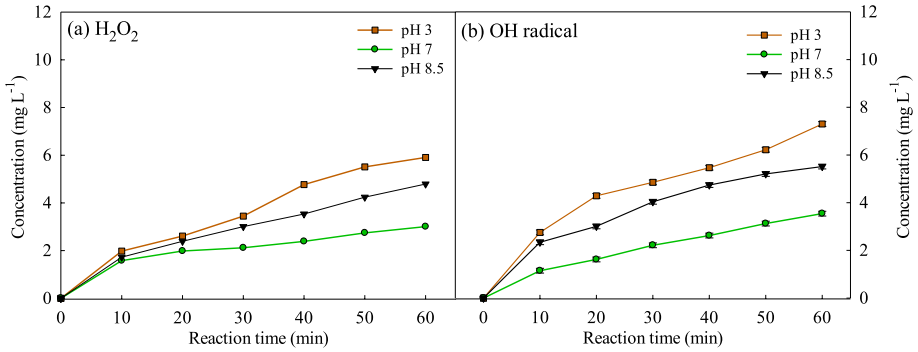

Fig. 1 Generation of (**a**) H_2O_2 in EO and (**b**) •OH in EF over 60 min at pH 3, 7, and 8.5 with a CD of 10 mA $cm.^{-2}$ (Anode: BDD, Cathode: Graphite felt, 20 mM Na_2SO_4, 3 mM $FeSO_4$ in EF)

In BDD-EF and BDD-EO tests, EOM suspensions with and without IOM at the designed DOC concentration of 6 ± 0.5 mg L^{-1} were prepared first, followed by the addition of Na_2SO_4 and $FeSO_4{\cdot}7H_2O$ as previous electrochemical oxidations test, then diluted to 1 L. The CD applied was at 10 mA cm^{-2}, and the operational pH was adjusted to 3. Subsequently, before both BDD-EO and BDD-EF tests, the prepared AOM suspensions were mixed for 10 min to reach a dissolved oxygen level of approximately 8 mg L^{-1}. Each BDD-EF and BDD-EO test was performed for 1 h under intensive mixing, and 30 mL of the oxidized sample was withdrawn every 10 min for subsequent analysis.

2.4 Characterization of AOM

The AOM fluorophore was characterized using a fluorescent spectrophotometer (RF-6000, Shimadzu, Japan) with a subsequent scanning excitation wavelength (Ex) from 200 to 500 nm and emission spectra (Em) in the range of 250 to 550 nm. Each test was tailored to four specific regions based on each EEM peak with excitation/emission (Ex/Em) wavelengths: soluble microbial product-like (SMPL) (region I 250–340/280–380 nm), aromatic protein-like (APL) (Region II 200–250/280–380 nm), humic acid-like (HAL) (Region III 250–400/380–550 nm), and fulvic acid-like (FAL) (Region IV 200–250/380–550 nm), as previously described [26, 27]. These regions were measured according to the AFI. Each component in the analysis of fluorescent organics was determined to investigate the organic degradation of EOM suspensions and EOM-IOM mixture. The fluorescent signal depends on the presence of fluorophores and different organic matter fractions. This method relies on the relative assessment of organic matter composition or chemical structures based on fluorescent characteristics.

The DOC samples were measured using a total organic carbon analyzer (TOC-L, Shimadzu, Japan). A UV–Vis spectrophotometer (Genesys.™ 10S, Thermo Scientific, USA) was used to measure UV absorbance at 254 nm. The reduction ratios of DOC and UV_{254} were calculated using Eq. (1)

$$\text{Reduction ratio (\%)} = \frac{N_o - N_t}{N_o} \times 100\% \tag{1}$$

where N_o represents the initial value of the original AOM suspension and N_t is the value of the treated samples after BDD-EO and BDD-EF. The degradation constant of DOC and UV_{254} by BDD-EO and BDD-EF was assumed as a first-order condition and determined using Eq. (2), adapted from previous study [28].

$$\text{Ln}\left(\frac{C_t}{C_o}\right) = -kt \tag{2}$$

where C_t is the treatment concentration after EO and EF, C_o is the initial concentration (mg L^{-1}), t is the electrolysis time (min), and k is the degradation constant (min^{-1}).

2.5 Fractionation of organic MW

AOM samples obtained after the EO and EF treatment for MW analysis were conducted using size exclusion high-performance liquid chromatography (HPLC-SEC) (LC-2030C 3D plus, Shimadzu, Japan) connected with sequential online detectors consisting of a photodiode array detector (Shimadzu). A chromatographic column (8 × 300 mm Protein KW-802.5, Shodex, USA), a hydrophilic hydroxyl group covered by porous silica-based gel filtration chromatography, was used for size-exclusion chromatography. The effluent containing phosphate buffer (20 mM K_2HPO_4; pH 6.8 ± 0.1) was filtered through a 0.2 μm MCE membrane filter (Advantec, Japan). The flow rate of the column was set to approximately 1 mL min^{-1}. Polyethylene glycol was used as a standard to calibrate the system, ranging from 300 to 110,000 g mol^{-1}. The "Log-Normal-4 Area" model was

selected as the peak fitting technique, PeakFit (version 4.12, Systat Software Inc., CA, USA), to resolve the overlapping peaks in HPLC-SEC chromatograms.

2.6 Protocol of DBPFP quantification

In this study, brominated DBPs are neglected because bromide was not introduced into the suspensions. The formation of halogenated DBPs was investigated to extract two THMs – trichloromethane (TCM) and trichloronitromethane (TCNM), two haloacetonitriles (HANs) – dichloroacetonitrile (DCAN) and trichloroacetonitrile (TCAN), two haloketones (HKs) – 1,1-dichloroacetone (1,1-DCK) and 1,1,1-trichloroacetone (1,1,1-TCK), and three HAAs – mono chloroacetic acid (MCAA), dichloroacetic acid (DCAA), and trichloroacetic acid (TCAA). Before extraction, the DOC sample was quantified following 5:1 (Cl_2:DOC) ratio to calculate the yield of DBPs after a 7-d chlorination procedure. THMs, HANs, and HKs extraction followed USEPA method 551.1 [29]. A 30 mL sample was transferred to a 40 mL glass vial containing 10 g anhydrous sodium chloride, followed by the addition of 3 mL methyl tert-butyl ether. For the measurement of HAAs, a modified version of the USEPA method 552.3 [30] was employed, which involved acidification of the water samples with H_2SO_4 to adjust the pH to less than 0.5, followed by adding 2 mL of acidic methanol and incubating at 55 °C for 2 h for methylation. After this process, the samples were mixed with 5 mL Na_2SO_4 and 2 mL saturated $NaHCO_3$. A gas chromatography-electron capture detector (GC/ECD) was used to analyze all extracted DBP samples. The GC/ECD was equipped with a column of 30 m × 0.25 mm × 0.25 µm (DB-1701, Agilent, USA). The method detection limit of each DBP compound was determined in the range of 0.01 to 0.23 µg L^{-1}.

3 Results and discussion

3.1 H_2O_2 and •OH generation during BDD-EO and BDD-EF processes

In this study, the production of H_2O_2 via BDD-EO and the generation of •OH with the addition of 3 mM Fe^{2+} as catalyst at BDD-EF reaction were examined in the absence of AOM suspensions due to the immediate reaction with the organic matter could present in suspensions. This test was conducted at CD of 10 mA cm^{-2} under varying pH conditions (3, 7, and 8.5) within 60 min. Figure 1 shows that the highest generation rate of H_2O_2 and •OH is achieved at pH 3, where the maximum amount can reach up to 4.3 and 18 mg L^{-1}, respectively. However, at pH 7 and pH 8.5, the least production of H_2O_2 and •OH is due to the deprotonation of intermediates during reactions, which reduces the efficiency of •OH and H_2O_2 formation [31]. This has echoed a previous study where 49 mg L^{-1} of H_2O_2 and 13 mg L^{-1} of •OH are generated within 1 h of BDD-EO at CD of 50 mA cm^{-2} [19]. It is anticipated that H_2O_2 and •OH generated by EO and EF at pH 3 become dominant active oxidants that could be applied to reduce the AOM as DBP precursors. A previous study demonstrated that controlling the sp^2/sp^3 ratio during the modification of the BDD electrode surface enhances the generation of H_2O_2 through the two-electron water oxidation reaction and the two-electron oxygen reduction reaction [32]. The investigations into active oxidants formed in EO and EF suggest that the EO and EF behaviors towards AOM degradation could be quite different.

3.2 Degradation of dissolved organic matter by BDD-EO and BDD-EF

The changes in DOC concentration at different AOM suspensions, including EOM and the mixture of EOM and IOM, by BDD-EO and BDD-EF at pH 3 were evaluated, as shown in Fig. 2a. The initial DOC concentration was conducted at 6 ± 0.5 mg L^{-1} for each test. The DOC concentration of EOM suspensions significantly reduces after 10 min and steadily decreases by BDD-EF within 1 h, reaching total reduction around 84% (Fig. S4). This superior decrease occurs due to the abundance of •OH generation, as depicted in Fig. 1b. Additionally, EOM suspensions possess a simple structure and pronounced hydrophobicity [4, 20], which facilitates the degradation in DOC by •OH. In contrast, BDD-EO shows a limited reduction in DOC in the EOM suspensions within 40 min, but it substantially decreases at 60 min. On the other hand, a similar trend in the DOC reduction of the EOM-IOM mixture by both BDD-EF and BDD-EO is observed even though BDD-EF has a higher DOC reduction. Meanwhile, the inference of first-order kinetic was quantified to determine the rate constant of DOC reduction during BDD-EO and BDD-EF. It shows that the degradation rate constant for EOM by BDD-EF reaches approximately 0.076 min^{-1} at 20 min, while a lower degradation rate constant appears as low as 0.014 min^{-1} for the IOM-EOM mixture by BDD-EF. However, the insignificant rate constant of DOC reduction is observed by BDD-EO in the range of 0.010–0.012 min^{-1} before 40 min regardless of IOM mixed with EOM. As the reaction time increases further to 60 min, a significant reduction in DOC occurs at 66%. Likewise, the reduction in UV_{254} for the EOM suspensions reaches 45% by BDD-EF after 1 h, whereas it merely causes a 30% reduction in UV_{254} for the IOM-EOM mixture, as shown in Fig. 2b. However, BDD-EO is ineffective in causing the UV_{254} reduction for EOM suspensions, accounting for around 30%, while a lower UV_{254} reduction is found at 20% for the IOM-EOM mixture. Meanwhile, the rate constant of UV_{254} reduction is observed for the EOM suspensions

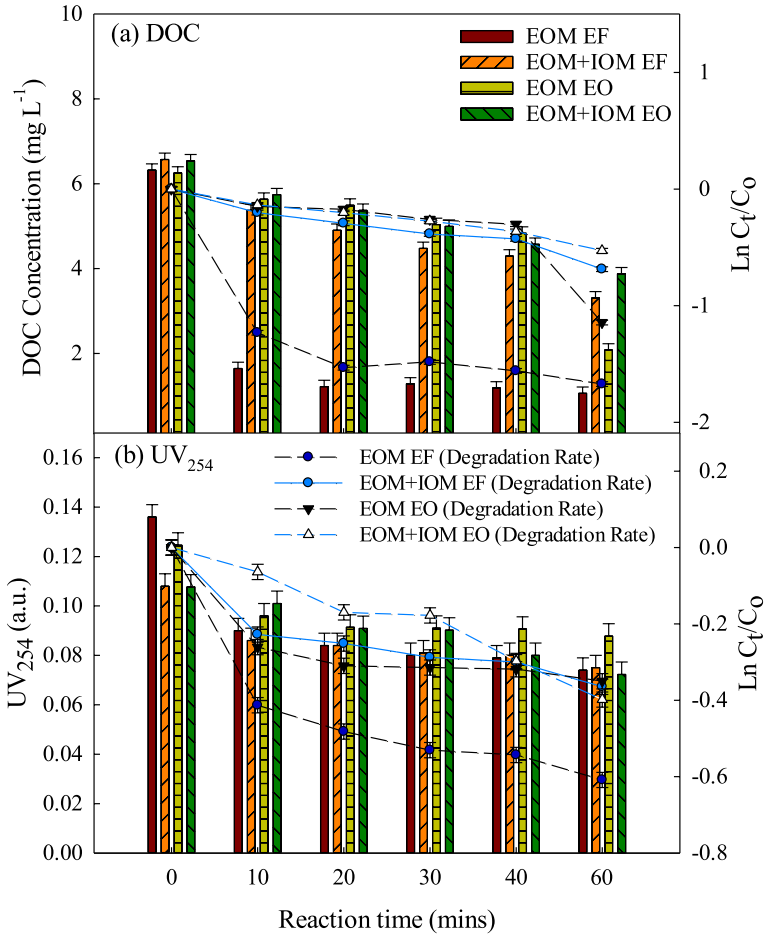

Fig. 2 Variations in (**a**) DOC concentration and (**b**) UV_{254} degradation in EOM suspensions and IOM-EOM mixtures by EO and EF at different reaction times (Anode: BDD, Cathode: graphite felt, pH 3, 20 mM Na_2SO_4, 3 mM $FeSO_4$ in EF, CD: 10 mA cm^{-2}, Initial DOC: 6 ± 0.5 mg $L^{-.1}$)

and EOM-IOM mixture. On the other hand, after 30 min, the BDD-EF exhibits a rate constant of UV_{254} reduction at 0.028 min^{-1} for the EOM suspensions, while the BDD-EF only reaches a half UV_{254} reduction rate for the IOM-EOM mixture.

Electrochemical oxidation is expected to play a significant role in the electro-combustion of organic matter into CO_2 [16]. Owing to the low level of •OH generated in BDD-EO, the effective combustion reaction does not proceed. In that case, the oxidation by H_2O_2 takes place during the low CD reaction instead of electro-combustion. A higher degradation rate constant for BDD-EF happens, possibly due to the majority of •OH can massively deform the electron-rich aromatic molecules and aliphatic substances into smaller fragments in the EOM suspensions. The decomposition of organics occurs through a series of oxidation reactions in which •OH radicals modify functional groups in organic molecules, ultimately leading to their transformation into simpler molecules [6]. Electrochemical methods for purifying organic molecules may be improved by employing anodes with greater overpotential for the generation of oxygen. BDD which possess this particular characteristic, facilitates the electro-oxidation of organic substances through hydroxyl radical generation and minimizes the competing process of oxygen evolution [19, 32]. Thus, BDD-EF causes a more effective DOC reduction by electro-combustion for MA-derived AOM.

Likewise, the enhanced reduction in UV_{254} by BDD-EF for EOM suspensions could be attributed to the high reactivity between •OH and unsaturated bond functional groups that are more susceptible to oxidation, as reported previously [19]. A previous study has shown a notable decrease in UV_{254} as AOM reacts with •OH, indicating the majority of aromatic compounds are degraded by AOPs [33]. Additionally, a previous study has reported that •OH preferentially reacts with aromatic compounds or organic compounds with free electron pairs, such as nitrogen, in larger protein molecules from AOM components [6]. Although •OH is powerful

to degrade UV_{254}-rich EOM, the reactivity of •OH and EOM could worsen in the presence of IOM due to the increase in hydrophilicity, as reported previously [3]. The presence of IOM substances could react with high-MW EOM (biopolymers) to form layers in the mixed IOM-EOM suspensions [34], which could lower the reactivity between oxidants and AOM. Therefore, it reduces the degradation efficiency of AOM in the IOM-EOM mixture compared to EOM alone in either BDD-EO or BDD-EF process. In summary, the BDD-EF effectively degrades highly reactive organic compounds in EOM suspensions, while the inhibition of AOM degradation appears in the case of IOM-EOM mixture. In contrast, the BDD-EO can implement effective DOC reduction after a longer reaction time (60 min) even though the degradation of UV_{254}-based AOM is insignificant at such a condition. In other words, the BDD-EO and BDD-EF behave marked differences in AOM degradation.

3.3 Degradation of fluorescent organics by BDD-EO and BDD-EF

The fluorescent spectra of AOM suspensions were analyzed to understand the degradation of fluorescent compounds by BDD-EO and BDD-EF. Figures S5 and S6 show that the original AOM solution contains the majority of HAL substances before electrochemical oxidation. Regardless of the composition of AOM suspensions, both BDD-EO and BDD-EF can remove fluorophore substances within 60 min, especially for BDD-EF treatment on the EOM suspensions. However, the presence of IOM can inhibit the reduction of AFI in both BDD-EF and BDD-EO processes. The degradation of fluorescent compounds by H_2O_2 or •OH in an oxidation process can result in significant changes in their fluorescent spectra. The F-EEM spectra show a noticeable reduction in AFI for the BDD-EF treatment on AOM degradation.

The BDD-EO generates large amounts of H_2O_2 that selectively breaks down humic-acid like substances in EOM suspensions. At the same time, BDD-EF can cause the degradation of various fluorescent AOM through the majority of active OH radicals, as illustrated in Fig. 3. In the IOM-EOM mixture, the BDD-EO effectively degrades humic-like substances (HAL and FAL substances) to reach maximum AFI reduction at around 70%. In contrast, BDD-EF reduces most SMPL and APL substances, accounting for AFI reduction at 80 and 85%, respectively. As shown in Fig. 3b, HAL substances play a crucial role in influencing oxidation reactions with H_2O_2, leading to a predominant reduction in HAL substances in the BDD-EO process, which is slightly superior to the BDD-EF process. Although HAL substances are more prone to attract •OH, leading to various reactions such as hydroxylation and ring opening [35], various functional groups, including carboxyl, phenolic, and hydroxyl groups within cyanobacteria-derived AOM significantly react with •OH generated in

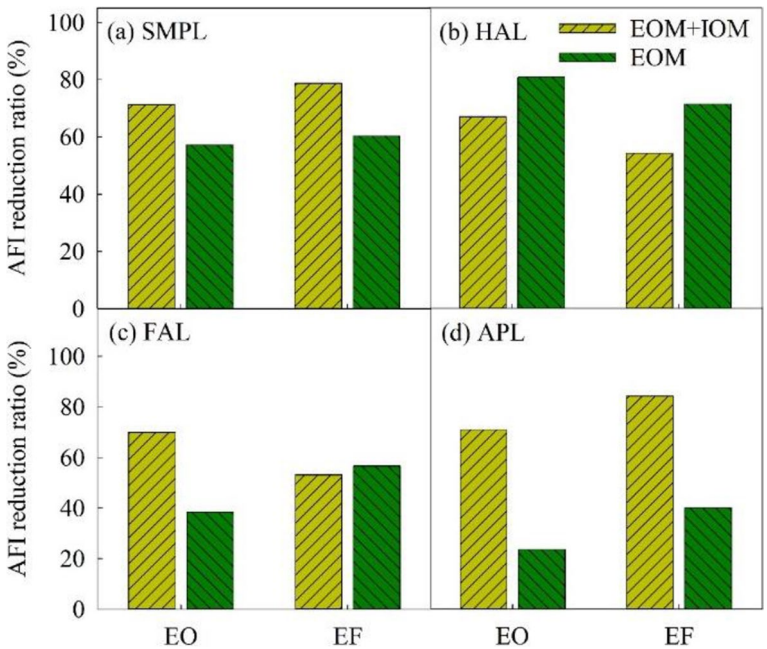

Fig. 3 The AFI reduction ratio from (**a**) soluble microbial product-like (SMPL), **b** humic acid-like (HAL), **c** fulvic acid-like (FAL) and **d** aromatic protein-like (APL) substances in EOM suspensions and IOM-EOM mixture after 1 h of EO and EF treatment. (Anode: BDD, Cathode: graphite felt, pH 3, 20 mM Na_2SO_4, 3 mM $FeSO_4$ in EF, CD: 10 mA cm^{-2}, Initial DOC: 6 ± 0.5 mg $L^{-.1}$)

the EF process, as reported previously [36], which could result in the pronounced reduction in biopolymers and proteins due to the weakened reactions between humic substances and OH radicals. Consequently, the BDD-EF preferentially degrades SMPL and APL substances, especially in the IOM-EOM mixture, instead of HAL and FAL substances compared to that by BDD-EO, as evidenced in Figs. 3a and b. The results in AFI variations indicate that BDD-EF can effectively minimize a wide range of fluorescent substances in response to the selectivity of •OH radicals towards AOM, especially for SMPL and APL substances; however, BDD-EO predominantly degrades humic-like substances as a result of preferential reactions between H_2O_2 and humic-like substances. These findings suggest that the degradation of MA-derived AOM by either BDD-EO or BDD-EF is subject to the composition of fluorescent compounds.

3.4 MW distribution profiles of EOM and IOM-EOM suspension by BDD-EO and BDD-EF

To further investigate the molecular degradation signature of AOM in the case of EOM suspension alone and the IOM-EOM mixture, the MW distribution profiles of EOM suspensions and IOM-EOM mixture by BDD-EO and BDD-EF were fractionated, as shown in Fig. 4. Before treatment by BDD-EO and BDD-EF, the EOM suspensions and IOM-EOM mixture have a similar feature peak in the biopolymers areas ($>10^4$ Da), humic substances (10^3–10^4 Da), and low-MW substances ($<10^3$ Da), whereas IOM only have low-MW substances ($<10^3$ Da).

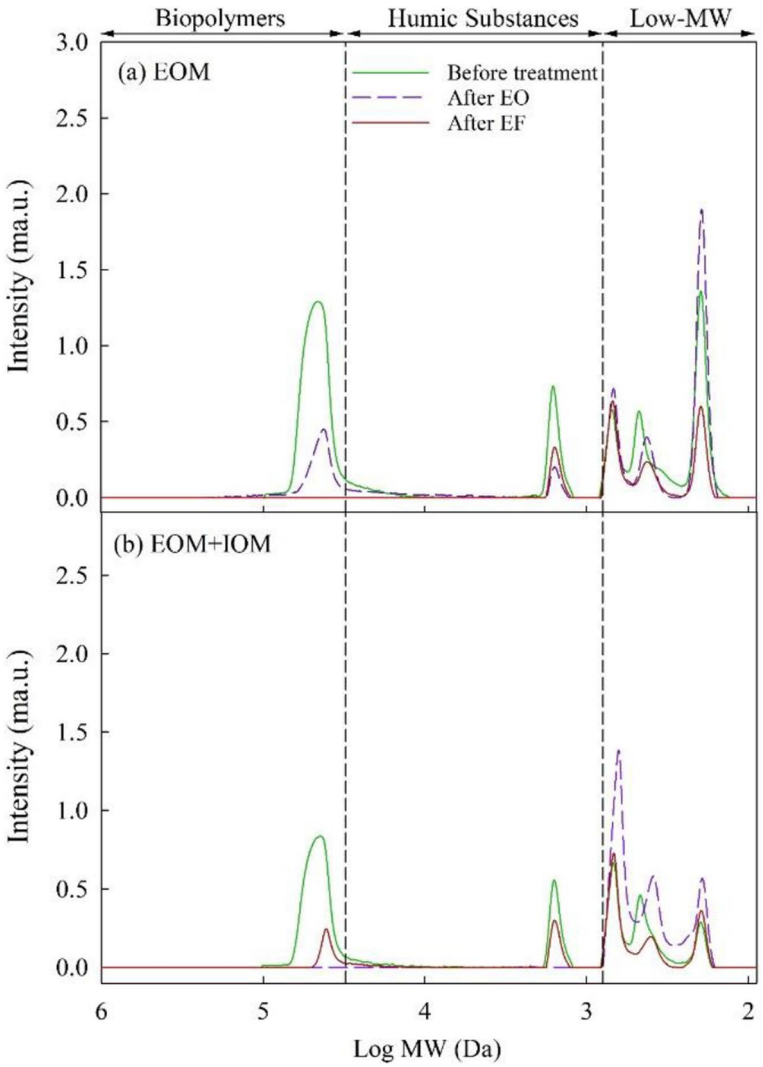

Fig. 4 Molecular weight distributions of (**a**) EOM suspensions and **b** IOM-EOM mixture before and after EO and EF treatment (Anode: BDD, Cathode: graphite felt, pH 3, 20 mM Na_2SO_4, 3 mM $FeSO_4$ in EF, CD: 10 mA cm^{-2}, Initial DOC: 6 ± 0.5 mg $L^{-.1}$)

The appearance of several peaks in the low-MW region indicates the presence of low-MW acids, predominantly hydrophilic molecules such as acetic and lactic acid, as reported previously [5]. In the case of EOM alone, the BDD-EF exhibits much more intensity reduction in each peak in the fraction of biopolymers, humic substances, and low-MW substances compared to BDD-EO owing to the stronger degradation ability of •OH in comparison with H_2O_2. However, in the case of the IOM-EOM mixture, the BDD-EO behaves a more substantial reduction in the peak intensities of biopolymers and humic substances. Meanwhile, the multiple peak intensities of low-MW substances increase in both cases where the degradation of humic substances by BDD-EO is superior to that by BDD-EF, which echoes the higher reduction in HAL substances in the BDD-EO process in Fig. 3b. Previous studies have elucidated that AOM containing N-organics compounds derived from biopolymer that could rapidly react with H_2O_2 [2, 37], which contributes to the degradation of biopolymers in the IOM-EOM mixture during the BDD-EO process. At such a condition, high-MW substances, including biopolymers and humic substances, are effectively decomposed into low-MW substances by electro-conversion [19, 32], as shown in Fig. 4b. In contrast, BDD-EF evenly behaves the degradation of various AOM in the EOM suspensions and IOM-EOM mixture by electro-combustion [38], which lowers the magnitude of low-MW substances, especially at EOM alone. In the presence of IOM, the AOM degradation is inhibited due to worsened reactivity induced by hydrophilic and low-MW substances, as shown in Fig. S7. The findings in the molecular degradation of AOM suggest that BDD-EO favors degradation of the molecules of biopolymers and humic substances to low-MW substances as well as BDD-EF preferentially degrades a broad spectrum of AOM evenly to a lower level of concentration instead.

3.5 Minimization of halogenated DBPs precursors by BDD-EO and BDD-EF

Halogenated DBP formation potential (DBPFP) is mainly subjected to the composition of AOM-derived DBPs precursors in oxidation processes [8]. Figure 5 shows the reduction of total DBPFP by BDD-EO and BDD-EF for the EOM suspensions alone and the IOM-EOM mixture. The BDD-EF exhibits much better total DBPFP reduction at EOM alone than BDD-EO, particularly in the inhibition of THMFP and HAAFP. However, BDD-EO implements a slightly superior reduction in total DBPFP in the case of the IOM-EOM mixture. A marked difference in various halogenated DBPs reductions between the EOM suspensions and IOM-EOM mixture is observed in Fig. S8. The BDD-EF can minimize TCM yields at approximately 72% in the process of THMs formation and the yields of DCAA and MCAA at approximately 94% for EOM suspensions. In contrast, in the case of the IOM-EOM mixture, the BDD-EO induces a similar reduction of MCAA at 96%, whereas the yields of TCM are only slightly reduced.

The variations of DBPFP reduction are associated with the remaining AOM after the BDD-EF and BDD-EO treatment. The remaining AOM are mostly HAL substances after BDD-EF and BDD-EO processes, as shown in Fig. S6, contributing to DBP formation potential. Humic and low-MW substances dominate the majority of DBP precursors, whereas biopolymers as hydrophobic compounds contribute to limited DBP formation potential, as previously reported [2, 26]. In addition, both humic substances and low-MW fractions in AOM have been identified as potential precursors of halogenated DBPs such as THMs and HAAs [37]. Thus, THMFP and HAAFP are dominant regardless of initial AOM composition. On the other hand, the lower DBPFP appears after BDD-EO, where HKFP is much less than that after BDD-EF, which could be attributed to the higher SUVA (UV_{254}/DOC) of remaining AOM after BDD-EO, as evidenced in Fig. 1.

Moreover, Fig. 6 illustrates the specific DBPFP variations, including THMs (TCM, TCNM), HAAs (MCAA, DCAA, and TCAA), HANs (TCAN, DCAN), and HKs (1,1-DCK and 1,1,1-TCK) originated from the EOM and IOM-EOM mixture before and after BDD-EO and BDD-EF. After either EO or EF treatment, specific DBPFP decreases as EOM is presented alone, whereas there is an increase in specific DBPFP in the IOM-EOM mixture. These results indicate that BDD-EO or BDD-EF treatment preferentially degrades non-DBP precursors in the case of the IOM-EOM mixture, even though BDD-EF is effective in DOC reduction. Previous studies have also indicated that IOM with the majority of low-MW substances, has a more significant potential to be DBP precursors than EOM [4, 8]. Most remaining AOM belong to low-MW substances after EO and EF, where the specific DBPFP is much higher than that without electrochemical oxidation for the IOM-EOM mixture due to a lower level of remaining DOC and higher DBPFP. Additionally, based on the toxic potency calculation described previously [39], the [DBP]/LC_{50} as a toxicity indicator was used to evaluate the toxicity of DBPs in this study. The higher the [DBP]/LC_{50} ratio is, the higher total toxicity the DBPs exhibit. As shown in Fig. 7a, the ratio of [DBP]/LC_{50} is reduced in the post-chlorination of EOM suspensions after EO and EF treatments, especially for EF where the ratio of [DBP]/LC_{50} substantially decreases

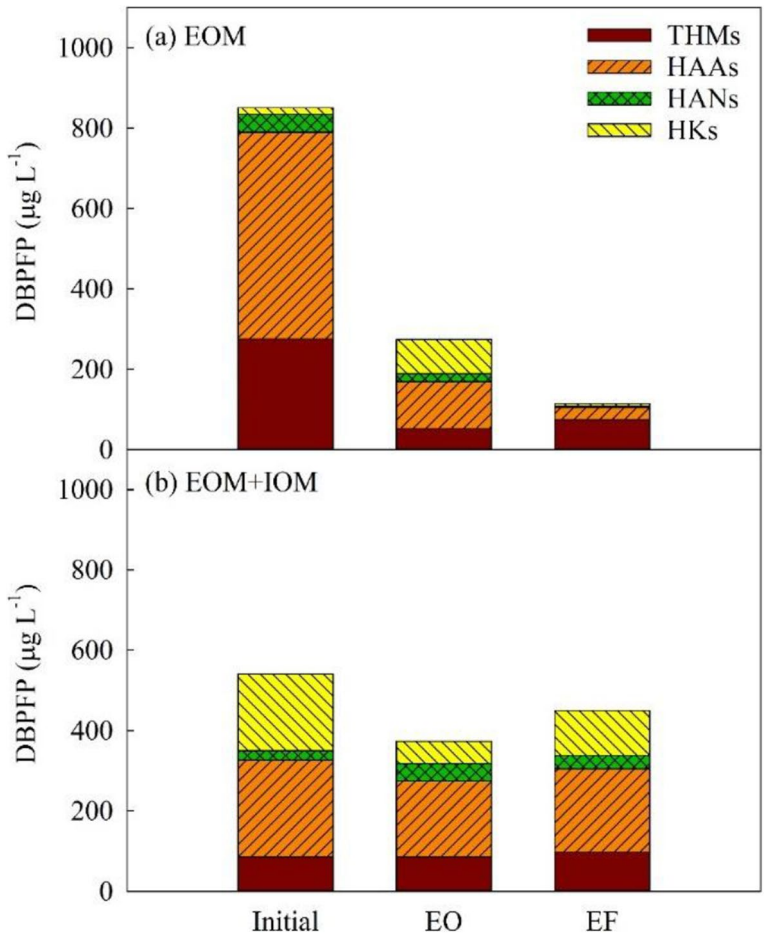

Fig. 5 DBPFP Variations in (**a**) EOM and **b** IOM-EOM mixture by EO and EF (Anode: BDD, Cathode: graphite felt, pH 3, 20 mM Na_2SO_4, 3 mM $FeSO_4$ in EF, CD: 10 mA cm^{-2}, Initial DOC: 6 ± 0.5 mg L^{-}.^{1})

from 0.011 to 0.001. However, in the case of IOM-EOM mixture, the ratio of [DBP]/LC_{50} increases slightly regardless of EO or EF treatments, as indicated in Fig. 7b. The marked difference in the toxicity between EOM suspensions and IOM-EOM mixture after EO and EF could be contributed by the dominant toxicity driver-DCAN. The toxicity contributions from DCAN in the case of EO and EF are pronounced, accounting for approximately 90% for EO and 75% for EF, respectively, as shown in Fig. 7. The formation of DCAN has been proven its higher toxicity potential compared to the generation of other DBP compounds [39]. The increase in DCAN formation is essentially caused by the presence of •OH that react with non-nitrogenous aromatic compounds to form phenolic compounds, ultimately leading to the formation of nitrogenous DCAN precursors [40]. Despite the DBPFP can be effectively attenuated by EO and EF in the case of IOM-EOM mixture, the EO and EF processes can increase the levels of toxicity of DBPs formed in post-chlorination. For EOM alone, EF is more effective to mitigate the toxicity tendency of DBP compounds than EO even though EF possesses a higher DBPFP.

3.6 Molecular degradation signature of MA-derived DBPs precursors by BDD-EO and BDD-EF

Based on the findings of this study, the molecular degradation signature of MA-derived AOM by BDD-EO and BDD-EF at pH 3 and CD 10 mA cm^{-2} in the case of EOM alone and IOM-EOM mixture is proposed, as depicted in Fig. 8. It reveals that H_2O_2 generation favors the degradation of organic matter via direct electron transfer or electro-conversion in the EO process, while •OH is responsible for deforming organic matter via electro-combustion in the EF process [38]. With BDD-EO treatment, it is able to generate abundant H_2O_2 and then decompose some of high-MW molecules, such as biopolymers and humics (i.e., HAL substances), into a certain amount of low-MW substances (< 10^3 Da) at EOM suspensions alone, while the high-MW molecules (> 10^3 Da) are comprehensively degraded into much more low-MW

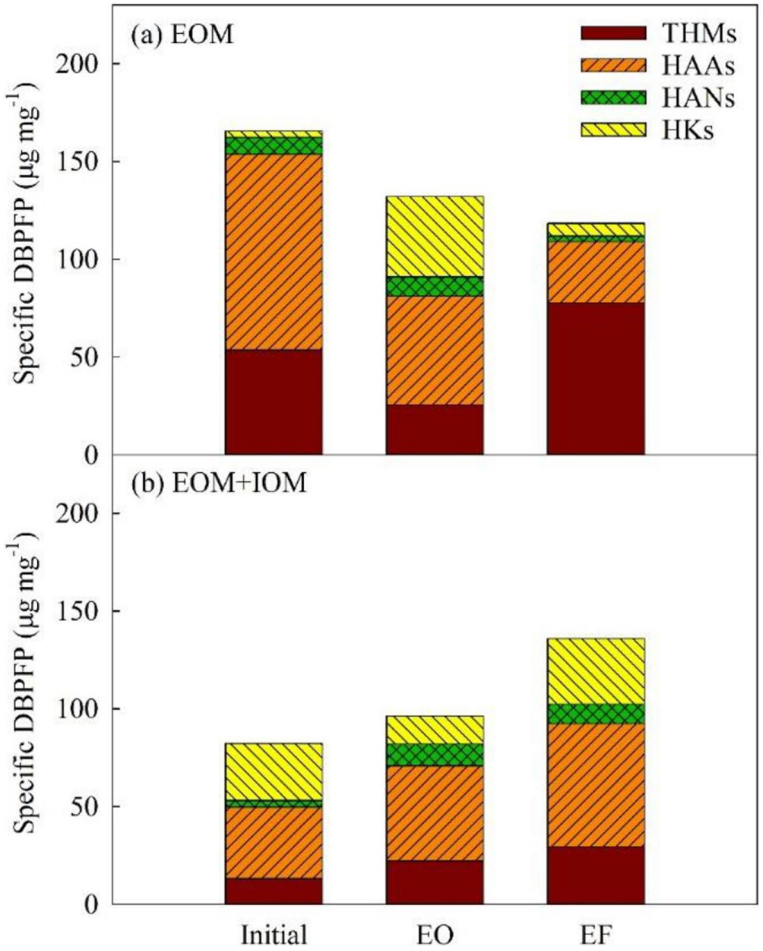

Fig. 6 Specific DBPFP variations in (**a**) EOM and **b** IOM-EOM mixture by EO and EF (Anode: BDD, Cathode: graphite felt, pH 3, 20 mM Na_2SO_4, 3 mM $FeSO_4$ in EF, CD: 10 mA cm^{-2}, Initial DOC: 6 ± 0.5 mg L^{-}.^{1})

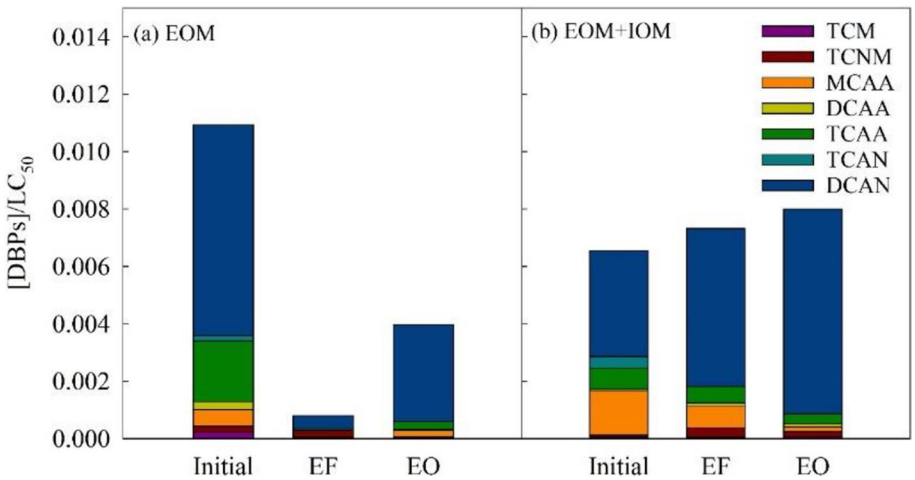

Fig. 7 Total toxic potency-weighted DBP concentrations derived from the chlorinated samples of (**a**) EOM and **b** EOM-IOM mixture before and after EF and EO treatment. (Anode: BDD; Cathode: Graphite felt; CD: 10 mA cm^{-2}; Initial DOC: 6 ± 0.5 mg L.$^{-1}$). The toxic potency of each DBP compound was determined according to the values provided in the previous studies [39]

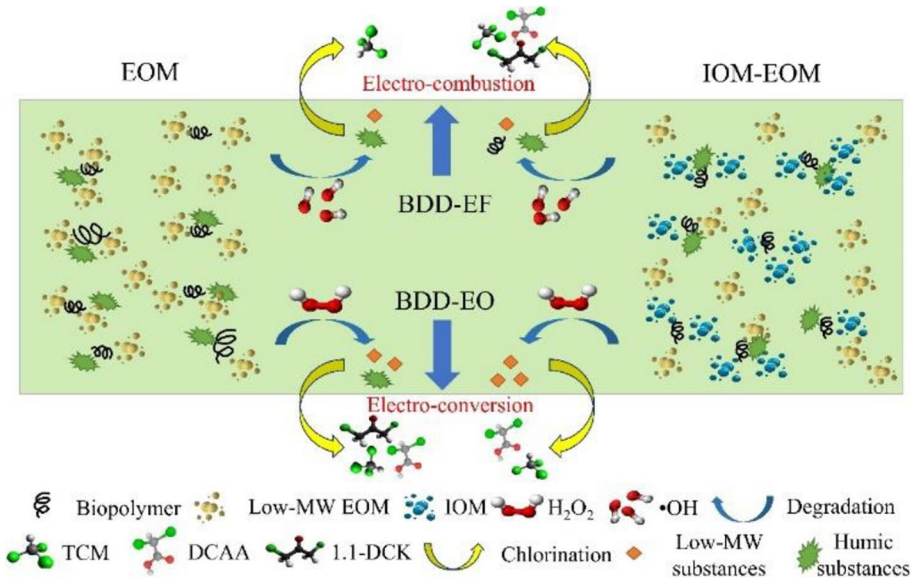

Fig. 8 Molecular degradation signature of AOM by BDD-EF and BDD-EO in the case of EOM and IOM-EOM mixture

substances in the case of IOM-EOM mixture, as proven in Fig. 4. In contrast, BDD-EF is effective to generate the majority of •OH and then evenly deform various AOM to lower their quantities at EOM suspensions alone, but the degradation of high-MW and low-MW substances is inhibited in the case of IOM-EOM mixture, as evidenced by the variations in degradation rate constants in terms of DOC and UV_{254} in Fig. 1. The remaining humic substances and low-MW substances after either BDD-EO or BDD-EF treatment would act as DBPs precursors and cause variations in DBPFP, as shown in Fig. 5. In the case of EOM suspensions, BDD-EO can cause a pronounced reduction in HAAs precursors (i.e., DCAA) and an effective reduction in THMs precursors (i.e., TCM), accompanying the remaining TCM, DCAA and 1.1-DCK. However, the decrease in HAAs and THMs precursors would be inhibited, as evidenced by the majority of remaining TCM and DCAA. By contrast, BDD-EF is powerful to decompose HAAs and THMs precursors at EOM suspensions alone, leading to remaining TCM. In the case of IOM-EOM mixture, most HAAs and THMs precursors remain after BDD-EF treatment and then cause a significant increase in TCMFP, MCAAFP, and 1.1-DCKFP. In summary, BDD-EO and BDD-EF exhibit a marked difference in the molecular degradation of AOM, depending on the AOM composition, which is significant in response to their corresponding DBPFP.

4 Conclusions

Electro-oxidation (EO) and electro-Fenton (EF) driven by BDD-based electrolysis have demonstrated remarkable effectiveness in the degradation of MA-derived AOM depending on its molecular composition. With 1 h electrochemical oxidation reaction by controlling CD at 10 mA cm^{-2} and pH at 3, the majority of •OH generated by BDD-EF can cause a significant reduction in DOC level up to 84% along with 45% reduction in UV_{254} for EOM suspensions alone. At the same time, BDD-EO merely reaches the maximum DOC reduction at 66% and UV_{254} reduction at 30%. However, the complexity of organic compounds in the IOM-EOM mixture inhibits the AOM degradation to increase the amounts of remaining organics in the process of BDD-EF and BDD-EO. Interestingly, there are marked differences in the degradation of fluorescent compounds and varied MW substances by BDD-EO and BDD-EF. BDD-EO with abundant H_2O_2 preferentially degrades humic compounds (i.e., HAL substances) regardless of AOM composition. BDD-EF with dominant •OH can decompose various AOM molecules, especially for reducing SMPL and APL substances in the IOM-EOM mixture. With BDD-EO treatment, it is effective in decomposing some high-MW compounds ($> 10^3$ Da), such as biopolymers and humics (i.e., HAL substances), into certain amounts of low-MW substances ($< 10^3$ Da) by electro-conversion at EOM suspensions alone. By

contrast, much more low-MW substances appear in the case of IOM-EOM mixture due to a significant decomposition of high MW fractions. The BDD-EF effectively deforms various AOM molecules to lower their quantities by electro-combustion at EOM suspensions alone. However, the degradation of high-MW and low-MW substances is significantly inhibited in the case of the IOM-EOM mixture. The corresponding DBPFP of the degraded AOM is subject to the quantity of remaining HAL substances and low-MW fractions, leading to a substantial reduction of HAAFP by either BDD-EO or BDD-EF in the case of EOM alone. However, the reductions in HAAFP and THMFP are significantly inhibited in the case of the IOM-EOM mixture. After either BDD-EF or BDD-EO, specific DBPFP decreases as EOM presents alone, while the increase in specific DBPFP appears in the case of the IOM-EOM mixture where BDD-EO outcompetes the performance in lowing specific DBPFP compared to BDD-EF. As IOM mixed with EOM, the toxicity tendency of corresponding DBP compounds formed in the post-chlorination would increase regardless of EO or EF, while the DBP-derived toxicity would be attenuated effectively for EOM alone, especially for EF. In summary, electrochemical oxidation processes, such as EO and EF, effectively reduce cyanobacteria-derived DBP precursors and the toxicity of DBPs formed in the post-chlorination for EOM suspensions. Instead, IOM releasing into EOM suspensions greatly impacts the degradation of DBP precursors by EO and EF and the toxicity of corresponding DPB compounds.

Supplementary Information

The online version contains supplementary material available at https://doi.org/10.1186/s42834-024-00235-9.

Supplementary Material 1.

Authors' contributions

Credit: Jr-Lin Lin Conceptualization, Validation, Resources, Writing-Review & Editing, Funding Acquisition, Supervision; Angga Dheta Shirajjudin Aji Writing-Original Draft, Methodology, Investigation. Writing and Editing, Methodology, Formal Analysis, Data Curation; Fahrudin Sidik: Writing and Editing, Methodology, Formal Analysis, Data Curation.

Funding

Not applicable.

Data availability

The authors declare that the data supporting the findings of this study are available within the paper and its Supplementary Information files. Should any raw data files be needed in another format they are available from the corresponding author upon reasonable request.

Declarations

Ethics approval and consent to participate

This study did not involve human or animal subjects, thus ethical approval was not required.

Competing interests

The authors declare that they have no known competing financial interests or personal relationships that could have appeared to influence the work reported in this paper.

Author details

[1]Department of Environmental Engineering, Chung Yuan Christian University, Chung-Li 320314, Taiwan. [2]Department of Civil Engineering, Chung Yuan Christian University, Chung-Li 320314, Taiwan.

Received: 12 July 2024 Accepted: 13 November 2024
Published online: 22 November 2024

References

1. Leloup M, Pallier V, Nicolau R, Feuillade-Cathalifaud G. Assessing transformations of algal organic matter in the long-term: impacts of humification-like processes. Int J Mol Sci. 2015;16:18096–110.
2. Hua LC, Chao SJ, Huang C. Fluorescent and molecular weight dependence of THM and HAA formation from intracellular algogenic organic matter (IOM). Water Res. 2019;148:231–8.
3. Lin JL, Ika AR. Minimization of halogenated DBP precursors by enhanced PACl coagulation: The impact of organic molecule fraction changes on DBP precursors destabilization with Al hydrates. Sci Total Environ. 2020;703:134936.
4. Hua LC, Lin JL, Chen PC, Huang C. Chemical structures of extra- and intra-cellular algogenic organic matters as precursors to the formation of carbonaceous disinfection byproducts. Chem Eng J. 2017;328:1022–30.
5. Hua LC, Lai CH, Wang GS, Lin TF, Huang C. Algogenic organic matter derived DBPs: Precursor characterization, formation, and future perspectives – A review. Crit Rev Env Sci Tec. 2019;49:1803–34.
6. Hua LC, Huang C, Huang C. Insights on free radical oxidation and in-situ coagulation in PMS/Fe(II) process for the removal of algogenic organic matter precursors. Chem Eng J. 2022;446:136986.
7. Lin JL, Hua LC, Hung SK, Huang C. Algal removal from cyanobacteria-rich waters by preoxidation-assisted coagulation–flotation: Effect of algogenic organic matter release on algal removal and trihalomethane formation. J Environ Sci-China. 2018;63:147–55.
8. Lin JL, Nugrayanti MS, Ika AR, Karangan A. Removal of *Microcystis* Aeruginosa by oxidation-assisted coagulation: Effect of algogenic organic matter fraction changes on algae destabilization with Al hydrates. J Water Process Eng. 2021;42:102142.
9. Hua LC, Lin JL, Syue MY, Huang C, Chen PC. Optical properties of algogenic organic matter within the growth period of *Chlorella* sp. and predicting their disinfection by-product formation. Sci Total Environ. 2018;621:1467–74.
10. Zhang X, Ma Y, Tang T, Xiong Y, Dai R. Removal of cyanobacteria and control of algal organic matter by simultaneous oxidation and coagulation - comparing the H_2O_2/Fe(II) and H_2O_2/Fe(III) processes. Sci Total Environ. 2020;720:137653.
11. Wang X, Wang X, Mi J, Du Q, Wang Y, Chen W, et al. UV/H_2O_2/O_3 removal efficiency and characterization of algae-derived organic matter and odorous substances. J Environ Chem Eng. 2023;11:109128.
12. Wang X, Xiang P, Zhang Y, Wan Y, Lian H. The inhibition of Microcystis aeruginos by electrochemical oxidation using boron-doped diamond electrode. Environ Sci Pollut R. 2018;25:20631–9.
13. Meglic A, Pecman A, Rozina T, Leštan D, Sedmak B. Electrochemical inactivation of cyanobacteria and microcystin degradation using a boron-doped diamond anode — A potential tool for cyanobacterial bloom control. J Environ Sci-China. 2017;53:248–61.
14. Biswas B, Goel S. Electrocoagulation and electrooxidation technologies for pesticide removal from water or wastewater: A review. Chemosphere. 2022;302:134709.

15. Jiang B, Niu Q, Li C, Oturan N, Oturan MA. Outstanding performance of electro-Fenton process for efficient decontamination of Cr(III) complexes via alkaline precipitation with no accumulation of Cr(VI): Important roles of iron species. Appl Catal B Environ. 2020;272:119002.
16. Kondo T. Recent electroanalytical applications of boron-doped diamond electrodes. Curr Opin Electroche. 2022;32:100891.
17. Wenderich K, Nieuweweme BAM, Mul G, Mei BT. Selective electrochemical oxidation of H_2O to H_2O_2 using boron-doped diamond: an experimental and techno-economic evaluation. ACS Sustain Chem Eng. 2021;9:7803–12.
18. Targhan H, Evans P, Bahrami K. A review of the role of hydrogen peroxide in organic transformations. J Ind Eng Chem. 2021;104:295–332.
19. Long Y, Li H, Xing X, Ni J. Enhanced removal of Microcystis aeruginosa in BDD-CF electrochemical system by simple addition of Fe^{2+}. Chem Eng J. 2017;325:360–8.
20. Chu H, Yu H, Tan X, Zhang Y, Zhou X, Yang L, et al. Extraction procedure optimization and the characteristics of dissolved extracellular organic matter (dEOM) and bound extracellular organic matter (bEOM) from *Chlorella pyrenoidosa*. Colloid Surface B. 2015;125:238–46.
21. Macpherson JV. A practical guide to using boron doped diamond in electrochemical research. Phys Chem Chem Phys. 2015;17:2935–49.
22. Xu J, Natsui K, Naoi S, Nakata K, Einaga Y. Effect of doping level on the electrochemical reduction of CO_2 on boron-doped diamond electrodes. Diam Relat Mater. 2018;86:167–72.
23. Lim J, Hoffmann MR. Substrate oxidation enhances the electrochemical production of hydrogen peroxide. Chem Eng J. 2019;374:958–64.
24. Charbouillot T, Brigante M, Mailhot G, Maddigapu PR, Minero C, Vione D. Performance and selectivity of the terephthalic acid probe for OH as a function of temperature, pH and composition of atmospherically relevant aqueous media. J Photoch Photobio A. 2011;222:70–6.
25. Hou JT, Zhang M, Liu Y, Ma X, Duan R, Cao X, et al. Fluorescent detectors for hydroxyl radical and their applications in bioimaging: A review. Coordin Chem Rev. 2020;421:213457.
26. Lin JL, Sidik F. Harvesting of cyanobacteria and phosphorus by electrocoagulation-flocculation-flotation: Role of phosphorus precipitation in cell separations and organics destabilization. Water Res. 2024;259:121868.
27. Lin JL, Sidik F, Kang SF. Harvesting of microcells from cyanobacteria-laden water by energy-efficient electro-flocculation-flotation with aluminum hydrates. J Water Process Eng. 2023;52:103585.
28. Huang K, MacKay AA. Microcystin-LR degradation kinetics during chlorination: Role of water quality conditions. Water Res. 2020;185:116305.
29. USEPA. Method 551.1: Determination of Chlorination Disinfection Byproducts, Chlorinated Solvents, and Halogenated Pesticides/Herbicides in Drinking Water by Liquid-Liquid Extraction and Gas Chromatography With Electron-Capture Detection, Revision 1.0. Washington, DC: United States Environmental Protection Agency; 1995.
30. USEPA.Method 552.3: Determination of Haloacetic Acids and Dalapon in Drinking Water by Liquid-Liquid Microextraction, Derivatization, and Gas Chromatography with Electron Capture Detection, Revision 1.0. Washington, DC: United States Environmental Protection Agency; 2003.
31. Nakabayashi Y, Nosaka Y. The pH dependence of OH radical formation in photo-electrochemical water oxidation with rutile TiO_2 single crystals. Phys Chem Chem Phys. 2015;17:30570–6.
32. Espinoza-Montero PJ, Alulema-Pullupaxi P, Frontana-Uribe BA, Barrera-Diaz CE. Electrochemical production of hydrogen peroxide on Boron-Doped diamond (BDD) electrode. Curr Opin Solid St M. 2022;26:100988.
33. Deng Y, Zhao R. Advanced oxidation processes (AOPs) in wastewater treatment. Curr Pollut Rep. 2015;1:167–76.
34. Cai Q, Song K, Tian C, Wu X, Li Y, Huang Y, et al. Harvesting of *Microcystis* from waterbody by flocculation and filtration: the essential role of extracellular organic matters. J Water Process Eng. 2021;41:102053.
35. Lee D, Kwon M, Ahn Y, Jung Y, Nam SN, Choi IH, et al. Characteristics of intracellular algogenic organic matter and its reactivity with hydroxyl radicals. Water Res. 2018;144:13–25.
36. Fernandes TV, van Lier JB, Zeeman G. Humic acid-like and fulvic acid-like inhibition on the hydrolysis of cellulose and tributyrin. Bioenerg Res. 2015;8:821–31.
37. Zhou S, Zhu S, Shao Y, Gao N. Characteristics of C-, N-DBPs formation from algal organic matter: Role of molecular weight fractions and impacts of pre-ozonation. Water Res. 2015;72:381–90.
38. Liao AA, Spitzer M, Motheo AJ, Bertazzoli R. Electrocombustion of humic acid and removal of algae from aqueous solutions. J Appl Electrochem. 2008;38:721–7.
39. Wei X, Yang M, Zhu Q, Wagner ED, Plewa MJ. Comparative quantitative toxicology and QSAR modeling of the haloacetonitriles: forcing agents of water disinfection byproduct toxicity. Environ Sci Technol. 2020;54:8909–18.
40. Huang H, Zheng H, Jiao J, Lei Y, Zhou Y, Qiu J, et al. Trichloramine and hydroxyl radical contributions to dichloroacetonitrile formation following breakpoint chlorination. Environ Sci Technol. 2022;56:12592–601

Publisher's Note